Syntheses and crystal structures of mixed-ligand copper(II)–imidazole–carboxylate complexes

Syeda Shahzadi Batool [a*], William T. A. Harrison[b*], Quratulain Syed[c], Muhammad Salman Haider[d]

[a*]Department of Chemistry, Govt. Post Graduate Islamia college for women, Cooper Road, Lahore, Pakistan

[b*]Department of Chemistry, University of Aberdeen, Aberdeen AB24 3UE, Scotland

[c]Pakistan Council of Scientific and Industrial Research (***PCSIR***) Laboratories Complex Lahore, Pakistan

[d]Department of Chemical Engineering, [d]University of Gujrat, Gujrat, Pakistan

Abstract

The syntheses, characterization and crystal structures of the reaction products of Cu^{2+} ions with imidazole (Himz) and different aromatic carboxylates, *viz.*: $[Cu(Himz)_2(cinn)_2(H_2O)]$ (**1**), $[Cu(Himz)_2(paba)_2]$ (**2**) and $[Cu(Himz)_2(clba)_2]$ (**3**) ($cinn^-$= $C_9H_7O_2^-$, $paba^-$=$C_7H_6NO_2^-$, $clba^-$= $C_7H_4ClO_2^-$) are described and studied by spectroscopic (Uv-Visible, FTIR) measurements. The single-crystal X-ray diffraction analyses indicate that each complex is monomeric: the metal ion in (**1**) adopts square-pyramidal coordination geometry arising from two imidazole-nitrogen atoms, two cinnamate-O atoms and an apical aqua-O atom. Complexes **2** and **3** however, assume a square planar configuration, which is realized by the coordination of two N atoms of two imidazole moieties and two O atoms: in both complexes the imidazole moieties are *trans* to each other. TGA results indicate that upon heating, these complexes lose their carboxylate anions first, followed by removal of the imidazole molecules.

Keywords: Copper(II) carboxylate, 2-Chlorobenzoic acid; cinnamic acid; imidazole, *p*-aminobenzoic acid

---

*Corresponding authors (*E-mail: syeda_shahzadi_uet@yahoo.com, w.harrison@abdn.ac.uk)*

1. Introduction

Copper is not only a bio-relevant trace metal but also has coordination flexibility. In coordination with imidazole, which is a small sized ligand, it exhibits a structural variety in both coordination geometries and in number of imidazole moieties that are directly coordinated to copper(II) center. For instance, the complex $[Cu(dien)(imzH)](ClO_4)_2$ with diethylenetriamine (dien) has one imidazole group (imzH) attached to Cu(II) [1] while, the complex $[Cu(pic)_2(imzH)_2]$. $2H_2O$ has two Cu(II)-coordinated imidazole groups arranged in a cis disposition with each other [2]. Similary, monomeric complexes with three $[Cu(C_7H_4ClO_2)_2(imzH)_3]$ (where $C_7H_4ClO_2^{1-}$ = 2-chlorobenzoate) [3] four, $[Cu(imzH)_4Cl]Cl]$ [4], five $[Cu(imzH)_5](AsF_6)_2.\cdot H_2O]$ [4], and six $[Cu(imzH)_6](NO_3)_2]$ [5] imidazole ligands have been reported. Imidazole upon losing its N-bonded proton, can act as a bridging imidazolate (imz^{1-}) group, and can now coordinate to two Cu(II) centres through its two N atoms. Some imidazolate-bridged complexes include dimeric, $[(dien)Cu(\mu\text{-}imz)Cu(dien)](ClO_4)_3)$ [1], trimeric ($[Cu_3(H_2O)_4(imzH)_4(\mu\text{-}imz)_2(ox)_2]$) [6] and even polymeric complexes [7-8].

The copper(II)-imidazole based coordination chemistry has played a formative role in the design and construction of metal-organic hybrids comprising of N,N-chelating ligands and carboxylates. Our focus lies on metal-organic hybrids formed by discrete complexes. Designing of such inorganic-organic hybrids depends on coordinate covalent bonds, coordination geometry and most importantly on weak interactions that interweave the whole framework [9-10]. These may be simple hydrogen bonding interactions (H-N…H, H-O….H, C-H…O, C-H….Cl etc.), or π interactions for example π-π stacking interactions or N-H…π interactions. Copper(II)-imidazole-carboxylates having; SOD-dismutase activity [11], and DNA binding [12], antimicrobial [13], and magnetic [10] properties have been reported.

As a continuation of our research work on ternary Cu(II) complexes with N,N-chelating donor ligands and carboxylates [14-16], we report herein three ternary complexes of copper(II) ion, coordinated by imidazole and aromatic mono-carboxylates.

2. Experimental

2.1 Materials and Methods.

$CuCl_2.2H_2O$ and imidazole were purchased from Merck chemical company Germany, while cinnamic acid, *o*-chlorobenzoic acid, and *p*-aminobenzoic acid, methanol, DMSO and NaOH were purchased from Sigma-Aldrich, chemical company, and were used in the same condition as received.

2.2. Instrumentation

Elemental analyses for C H and N were carried out using a Perkin–Elmer 2400 II elemental analyzer. TGA was performed on TGA instrument Q500, USA in static air. FT-IR absorption spectra were recorded as KBr pellets with Avatar 360 E.S.P. Nicolet FT/IR spectrometer in the range of 4000–400 cm^{-1}. Uv-Visible spectrum was recorded in DMSO using a Mega-2100 Double Beam UV-Visible spectrophotometer.

2.3 Syntheses of complexes 1-3

For the synthesis of complexes **1-3**, a similar procedure was used involving the reaction of copper(II) salt with imidazole, followed by addition of carboxylate.

2.3.1 Synthesis of $[Cu(imzH)_2(cinn)_2(H_2O)]$ (1)

To a solution of $CuCl_2.2H_2O$ (0.171 g 1 mmol) in 30 cm^3 methanol, the imidazole solution (0.136 g, 2 mmols) in 10 cm^3 methanol was added in a drop-wise manner with continuous stirring. The resulting green solution was stirred for half an hour at room temperature. Then a mixture of cinnamic acid in methanol (0.296 g, 2 mmols) containing 20 drops of 1M $NaOH_{(aq)}$ was slowly added with continuous stirring. The resulting solution was heated at nearly 50ºC with stirring for one hour. The solution was filtered and kept at room temperature, and after seven days, crystals suitable for single crystal X-ray analysis were obtained. The blue crystals were washed in cold methanol and dried in the air. (Yield= 0.35g, 68%). Elemental analysis: calculated for $CuC_{24}H_{24}N_4O_5$: C, 56.29; H, 4.72; N, 10.94; Found: C, 56.28; H, 4.73; N, 10.95 FT-IR (KBr discs): 3448, 3246, 3151, 3129, 3068, 2965, 2865, 1654, 1638, 1581, 1565, 1546, 1495, 1447, 1391, 1368, 1331, 1293, 1267, 1248, 1200, 1175, 1140, 1111, 1098, 1072, 990, 979, 952, 881, 835, 774, 744, 714, 686, 657, 617, 586, 550, 487, 420 cm^{-1} Solubility: Slightly soluble in water, Soluble in DMSO, ethanol, methanol, acetone. λd–d (DMSO) = 634 nm

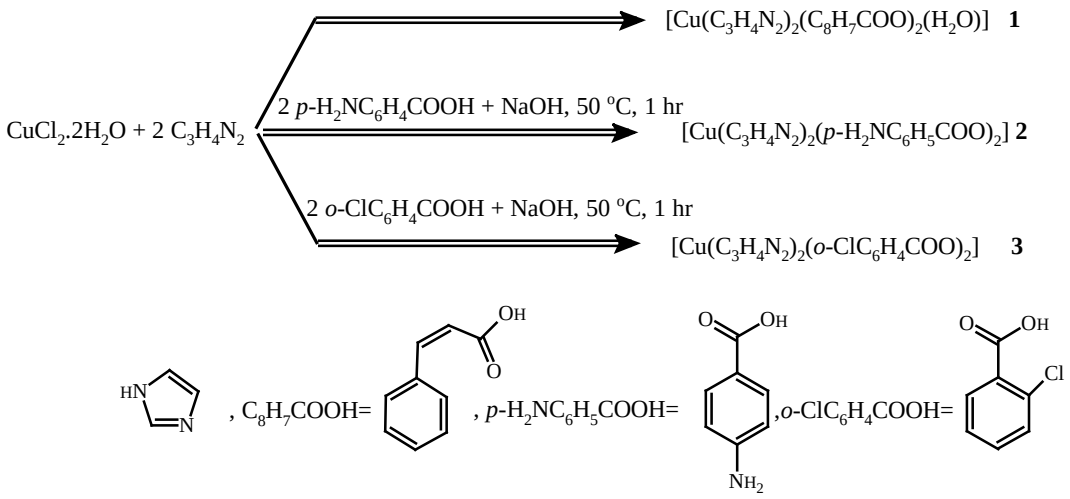

Scheme 1: Schematic sketch of synthetic procedure for complexes **1, 2** and **3**

2.3.2 Synthesis of [Cu(imzH)$_2$(paba)$_2$] (2)

The complex **2** was prepared by adopting a similar procedure as for **1**, involving addition of *p*-aminobenzoic acid (0.275 g, 2 mmols) in place of cinnamic acid. (Yield= 0.27g, 57%). Elemental analysis: calculated for $C_{20}H_{20}CuN_6O_4$: C, 50.89; H, 4.26; N, 11.87; Found: C, 50.87; H, 4.28; N, 11.89 FT-IR (KBr disc): 3441, 3351, 3298, 3142, 3062, 2954, 2849, 1633, 1608, 1588, 1538, 1512, 1496, 1437, 1394, 1329, 1305, 1262, 1245, 1180, 1142, 1128, 1112, 1095, 1067, 953, 943, 920, 874, 856, 803, 788, 758, 747, 730, 705, 665, 642 622, 611, 564, 506, 441, 415 cm^{-1}. Solubility: Slightly soluble in water, Soluble in DMSO, ethanol, methanol, acetone. λd–d (DMSO) = 652 nm

2.3.3 Synthesis of [Cu(imzH)$_2$(clba)$_2$] (3)

For complex 3, the same procedure was repeated using 2 mmols (0.313g) of 2-chlorobenzoic acid. (Yield= 0.34 g, 66%). Elemental analysis: calculated for $C_{20}H_{16}Cl_2CuN_4O_4$: C, 47.02; H, 3.15; N, 10.97; Found: C, 47.03; H, 3.16; N, 10.99. FT-IR (KBr disc): 3297, 3054, 2952, 2848, 2705, 2602, 1597, 1532, 1496, 1394, 1330, 1257, 1166, 1132, 1065, 944, 862, 775, 660, 611, 402 cm^{-1}. Solubility: Slightly soluble in water, Soluble in DMSO, ethanol, methanol, acetone. λd–d (DMSO) = 648 nm.

2.4. X-ray crystallography

Intensity data were collected for crystals of **1** (blue rod, 0.12 × 0.04 × 0.03 mm), **2** (blue shard, 0.06 × 0.02 × 0.01 mm) and **3** (dark blue block, 0.22 × 0.16 × 0.08 mm) at 100 K on a Rigaku Mercury CCD diffractometer using graphite monochromated MoKα radiation (λ = 0.71073 Å). The structures were routinely solved by direct methods and the structural models completed and optimized by refinement against $|F|^2$ with SHELXL-2014 [17]. The N- and O-bound H atoms were located in difference maps and either refined as riding atoms in their as-found relative locations or freely refined. The C-bound H atoms were geometrically placed and refined as riding atoms with C–H = 0.95 Å. The refinement for **2** resulted in an unexpectedly large peak of 3.40 *e* Å^{-3} in the final difference map, which, given its location, cannot correspond to an atom. Possible twinning was investigated and ruled out so we tentatively assign this to an artifact arising from less than optimal intensity data arising from a very small crystal. Key refinement details are shown in Table 1.

Table 1: Key crystallographic data for complexes **1**–**3**

	1	**2**	**3**
Empirical formula	$C_{24}H_{24}CuN_4O_5$	$C_{20}H_{20}CuN_6O_4$	$C_{20}H_{16}Cl_2CuN_4O_4$
M_r	512.01	471.96	510.81
Crystal system	Monoclinic	Monoclinic	Monoclinic
Space group	$P2_1/n$ (No. 14)	$P2_1/n$ (No. 14)	$P2_1/c$ (No. 14)
a (Å)	19.3917 (4)	7.45140 (10)	9.6726 (2)
b (Å)	5.6017 (2)	17.9911 (3)	19.9171 (4)
c (Å)	20.4802 (5)	7.8015 (2)	11.3056 (4)
β (°)	93.887 (2)	96.948 (2)	105.808 (3)
V (Å^3)	2219.57 (11)	1038.18 (3)	2095.65 (10)
Z	4	2	4
μ (mm^{-1})	1.029	1.092	1.333
ρ_{calc} (g cm^{-3})	1.532	1.510	1.619
Measured, unique refs.	15139, 5070	9347, 2624	37976, 5556
R_{Int}	0.045	0.029	0.078
$R(F)$ [$I > 2\sigma(I)$]	0.038	0.028	0.055
$wR(F^2)$ (all data)	0.092	0.078	0.158
min., max. $\Delta\rho$ (e Å^{-3})	–0.54, +0.43	–0.37, +0.39	–0.56, +3.40
CCDC deposition number	1543434	1543436	1543435

3. Results and Discussion

3.1. IR spectroscopy

The FTIR spectra of complexes **1-3** (Figs. S1-S3 of ESI), exhibit complex patterns of many characteristic peaks. For instance, in the FTIR spectrum of complex **1**, the absorption band at 3448 cm^{-1} is due to the ν(O-H) stretching vibration of coordinated water molecule [18]. The absorption peak at 3151 cm^{-1} is ascribed to ν(=C–H) stretch of alkenic moiety of cinnamate group, while its trans alkene bend is observed at 979 cm^{-1}. The complex **2** shows asymmetric ν_{as}(N–H) and symmetric ν_{s}(N–H) stretching vibrations of amino (-NH_2) group of *p*-aminobenzoate at 3441 cm^{-1} and 3351 cm^{-1}, respectively. The overtone of N-H bending vibration of NH_2 occurs as a shoulder at 3298 cm^{-1} [19]. The complex **3** shows characteristic ν(C-Cl) stretch at 775 cm^{-1}. The absorption bands at 3246 cm^{-1}, 3298 cm^{-1}, and 3297 cm^{-1} in (**1-3**) correspond to ν(=N–H) imidazolic stretches, respectively. The peaks at 3068 cm^{-1}, 3062 cm^{-1}, and 3054 cm^{-1}, are ascribed to ν(=C–H) aromatic stretching vibrations of **1-3**, respectively [20].

Upon coordination to Cu(II) center, new absorption bands appear at; 1638 cm^{-1} and 1391 cm^{-1}, for **1,** 1608 cm^{-1} and 1394 cm^{-1}, for **2,** and 1597 cm^{-1} and 1394 cm^{-1} for **3,** which correspond to the asymmetric [ν_{asym}(OCO)], and the symmetric [ν_{sym}(OCO)] stretching vibrations of the coordinated carboxylate groups, respectively. The large difference in ν_{as}(OCO) and ν_{s}(OCO) frequencies (Δν= 247 cm^{-1}, 214 cm^{-1}, and 203 cm^{-1} for **1-3**) is indicative of monodentate-O coordination of the carboxylate groups to the copper(II) center [18, 21]. The other absorption bands at 1581-1447 cm^{-1} correspond to ν(C=N) and aromatic ν_{s}(C=C) and stretching vibrations. The low-energy absorption bands in the range 611 cm^{-1}- 402 cm^{-1} can be associated to ν(Cu–O) and ν(Cu–N) stretching modes, respectively [22-23]. A comparison of the selected IR frequencies of free ligands including; imidazole [24], cinnamic acid [25], 4-aminobenzoic acid [26-27], and *o*-chlorobenzoic acid [28], with those of complexes **1-3** has been presented in Table S1 of ESI.

3.2 Uv-Visible spectroscopy

UV-Visible spectra of all the complexes were recorded in DMSO solution in the 200–1000 nm range. The complexes **1-3** exhibited three absorptions. The intense absorption bands at

higher energy, 268 nm and 210 nm for complex (**1**), 254 nm and 216 nm for complex (**2**), 252 nm and 213 nm for complex (**3**), are assigned to the intraligand π→π* and n→π* transitions [4]. A broad absorption band at 634 nm for complex (**1**) is due to the d-d transitions in square pyramidal complexes [29-31]. The visible absorption spectra also contain bands at 652 nm for (**2**) and 648 nm for (**3**), which are due to the copper(II) dxz; dyz→ dx^2-y^2transitions in a square-planar ligand field [32].

3.3 Thermal studies of complexes 1-3

Thermal analyses curve of the complex **1** (TG/DTA) is given in Fig. S4 of ESI. The thermal pattern of the complexes was studied up to 1000 ˚C in static air. For complex (1), the first stage of the thermal decomposition commences at 115 ºC and ends at 156 ºC with the elimination of a coordinated water molecule. The observed weight loss for this step was 3.52% while calculated was 3.52%. The second stage in the 156– 256 ºC temperature range involves the removal of two moles of the two cinnamato ligands (found 54.36%; calcd. 54.36%). The decomposition of two imidazole ligands occurs in the third stage between 256 ºC and 610 ºC (found 27.09%; calcd. 26.58%). The final decomposition product was CuO (found 15.03%; calcd. 15.54%).

The complex **2** is found to be thermally stable up to 194 ºC (Fig. S5 of ESI). The first stage of decomposition starts with the elimination of two *p*-aminobenzoate and progresses till 526 ºC. The weight loss during this stage amounts to 53.97% which is in agreement with the calculated value of 54.29%. No sharp decomposition curve had been observed for the subsequent step showing slow degradation of the imidazole yielding CuO. The TG-curve for the complex **3** (Fig. S6 of ESI) was studied upto 600 ºC. The first stage of the thermal decomposition in the 255– 548 ºC temperature range is associated with the removal of two *o*-chlorobenzoate groups. The observed weight loss for this step was 57.02% while calculated was 57.78%. The remaining fraction (calculated= 42.22%, observed= 42.98%) corresponds to two imidazole groups and one CuO.

3.4. Description of crystal structures 1-3

3.4.1. Crystal Structure of 1

The asymmetric unit of **1** is shown in Fig. 1 and consists of a single, neutral $[Cu(C_3H_4N_2)_2(C_9H_7O_2)_2(H_2O)]$ molecule in which two imidazole ligands (in a *trans* configuration) and two monodentate cinnamate^{1-} anions define the basal plane and a water molecule occupies the apical site of a square-pyramidal CuN_2O_3 coordination polyhedron. The apical Cu1–O5 bond length (2.2417 (16) A˚), is much longer than the basal bonds: key geometrical data are listed in Table 2. The dihedral angle between the Himz mean planes is 71.90 (7)° and the equivalent angle between the cinn$^-$ ring planes is 4.81 (16)°. The metal ion lies almost in the plane of its attached Himz ligands: deviation = 0.064 (3) Å for the N1 molecule and 0.002 (3) Å for the N3 molecule. It is notable that the uncoordinated oxygen atoms (O2 and O4) of the cinnamate carboxylate groups both point away from the coordinated O5 atom of the water molecule. In terms of the Himz ligands, both N2 and N4 are directed away from O5.

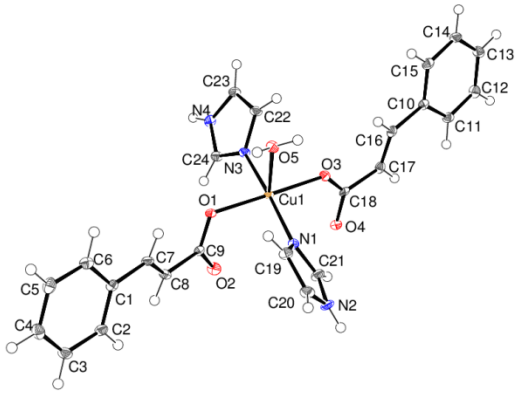

Figure 1: The molecular structure of **1** showing 50% displacement ellipsoids.

Table 2. Selected bond lengths (A˚) and angles (˚) for complex **1**

Bond Lengths			
Cu1–O3	1.9691 (14)	Cu1–N1	1.985 (2)
Cu1–N3	1.991 (2)	Cu1–O1	1.9927 (14)
Cu1–O5	2.2417 (16)	C9–O2	1.242 (3)
C9–O1	1.288 (3)	C18–O4	1.258 (3)
C18–O3	1.268 (3)		

Bond Angles			
O3–Cu1–N1	92.89(7)	N3–Cu1–O1	90.97(7)
O3–Cu1–N3	87.95(7)	O3–Cu1–O5	89.64(6)
N1–Cu1–N3	172.99(8)	N1–Cu1–O5	94.92(7)
O3–Cu1–O1	178.91(7)	N3–Cu1–O5	92.05(7)
N1–Cu1–O1	88.18(7)	O1–Cu1–O5	90.44(6)

In the crystal of **1**, O–HΛO and N–HΛO hydrogen bonds link the molecules. The O–HΛO links (Fig. 2) generate [010] chains, with adjacent molecules related by translational symmetry. The arrangement of the carboxylate groups in the molecule as noted above correlates with their optimal orientation to accept two O–HΛO links between each pair of molecules. By themselves, the N–HΛO bonds generate (10$\bar{1}$) sheets: the pendant benzene rings of the cinnamate^{1-} anions interdigitate between the layers: inversion-related C1 rings interact *via* aromatic π–π stacking [centroid–centroid separation = 3.7537 (14) Å]. Two weak C–HΛO bonds are also present (Table 3). Taken together, the intermolecular interactions in **1** lead to a three-dimensional network in the crystal.

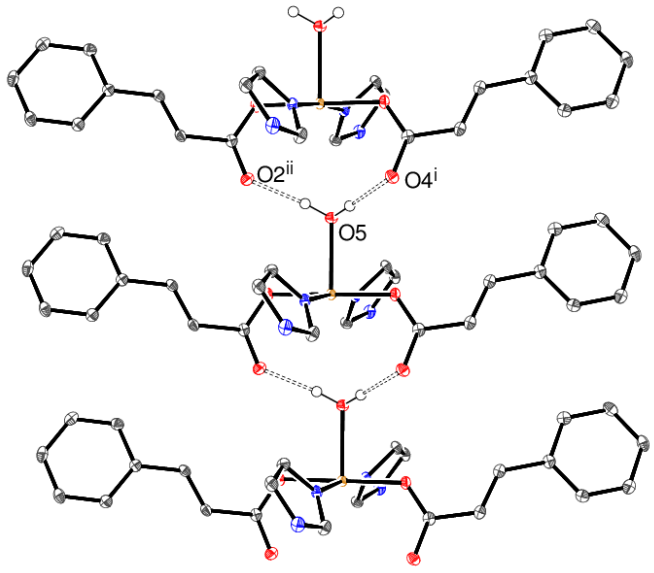

Figure 2: Fragment of the extended structure of **1** showing the formation of [010] chains linked by O–HΛO hydrogen bonds. Symmetry codes as in Table 3.

Table 3: Bond separations (Å) and bond angles (˚) in the complex (**1**)

Donor–H ….. Acceptor	D–H (Å)	H…A (Å)	D–H…A (Å)	D–H…A (°)
N2–H1nΛO4^{ii}	0.85	2.00	2.847 (3)	173
N4–H2nΛO1^{ii}	0.90	1.92	2.822 (3)	179
O5–H1wΛO2^{iii}	0.88 (3)	1.86 (3)	2.733 (2)	173 (3)
O5–H2wΛO4^{iii}	0.82 (3)	1.96 (3)	2.783 (2)	177 (3)
C19–H19ΛO2^{iii}	0.95	2.47	3.387 (3)	163
C21–H21ΛO4	0.95	2.49	3.220 (3)	133

Symmetry codes: (i) 1–*x*, 1–*y*, 1–*z*; (ii) ½–*x*, ½+*y*, 3/2–*z*; (iii) *x*, *y*–1, *z*.

3.4.2. Crystal Structure of 2

Selected bond distances, bond angles and hydrogen bonding details of complex **2** are given in Tables 4 and 5. Crystal packing diagram and the ORTEP drawing are given in Figs. 3 and 4.

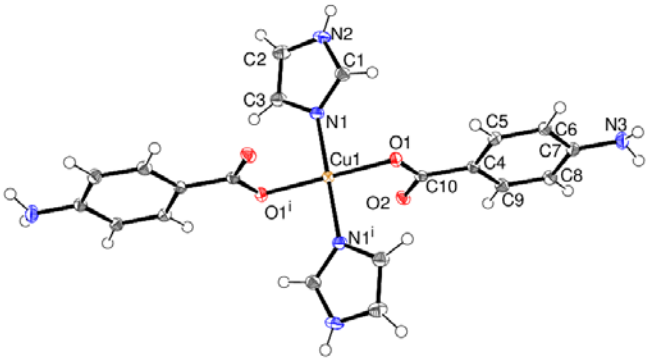

Figure 3: The molecular structure of **2** showing 50% displacement ellipsoids.

Symmetry code: (i) 1–*x*, 1–*y*, 1–*z*.

The asymmetric unit of **2** consists of an imidazole molecule, a *p*-aminobenzoate^{1-} anion and a copper(II) ion (site symmetry $\bar{1}$): the complete $[Cu(C_3H_4N_2)_2(C_7H_6NO_2)_2]$ complex is generated by crystallographic inversion symmetry (Fig. 3) to yield a *trans*-CuN_2O_2 square planar geometry for the metal ion (Table 4). The dihedral angles between the pairs of Himz planes and pairs of benzene ring planes are, of course, constrained to be 0° by symmetry; the dihedral angle between the unique Himz and benzene-ring planes is 73.19 (4)°. The copper(II) ion deviates from the imidazole ring plane by 0.191 (2) Å.

Table 4. Selected bond lengths (A˚) and angles (˚) for complex **2**

Bond Lengths			
Cu1-O1	1.9560 (10)	Cu1-N1	1.9785 (11)
C10-O2	1.2526 (17)	C10-O1	1.2826 (16)
Bond Angles			
O1-Cu1-O1	180.0	O1-Cu1-N1	90.33(4)
O1-Cu1-N1	89.67(4)	O1-Cu1-N1	89.67(4)
O1-Cu1-N1	90.33(4)	N1-Cu1-N1	180.0

Table 5: Bond separations (Å) and bond angles (˚) in the complex (**2**)

Donor–H ….. Acceptor	D–H (Å)	H…A (Å)	D–H…A (Å)	D–H…A (°)
N2–H1nΛO2^{i}	0.78(2)	2.03(2)	2.8142(16)	174(2)
N2–H2nΛπ^{ii}	0.87 (2)	2.84 (2)	3.6279 (14)	150.4(17)
N3–H3nΛO2^{iii}	0.89 (2)	2.24 (2)	3.0463 (17)	150.4 (17)
C2–H2Λπ^{iv}	0.95	2.59	3.4323 (16)	148

In the crystal of **2**, an unusual network of X–HΛπ interactions (X = C and N) generate undulating (101) sheets (Fig. 4), with the C4–C9 benzene ring accepting these interactions from both sides of the ring plane [H2nΛπΛH2 = 151°]. It is notable that the C–HΛπ bond is significantly shorter than the N–HΛπ link. In addition, N–HΛO hydrogen bonds are observed, which generate (010) sheets. Taken together, the intermolecular interactions in **2** lead to a three-dimensional network. Compared to **1** and **3**, there is no C–HΛO stacking interaction in the extended structure of **2**.

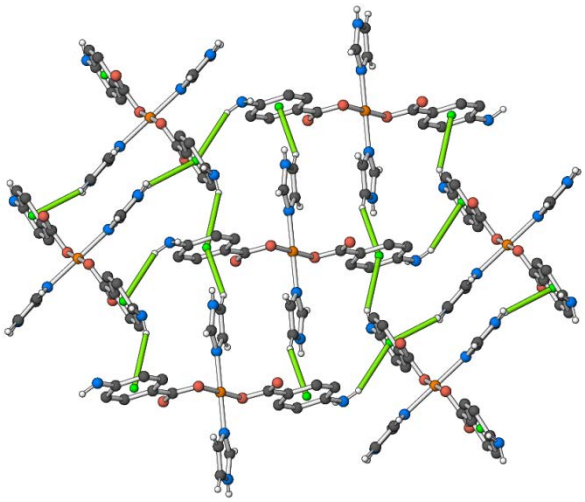

Figure 4: Fragment of an undulating sheet in the crystal structure of **2** with molecules connected by N–HΛπ and C–HΛπ links (green lines).

3.4.3. Crystal structure of 3

The asymmetric unit of **3** (Fig. 5) consists of a single $[Cu(C_3H_4N_2)_2(C_7H_4ClO_2)_2]$ molecule. In this case, a *trans*CuN_2O_2 square-planar geometry arises for the metal ion due to the coordination of two imidazole molecules and two monodentate 2-chlorobenzoate^{1-} anions. The dihedral angle between the Himz planes is 38.7 (2)° and that between the benzene ring planes is 62.03 (13)°. Compared to **1**, the metal ion in **3** shows a much larger deviation from the planes of the imidazole ligands: the deviations are 0.337 (5) Å and 0.298 (5) Å for the N1 and N3 molecules, respectively. Like **1**, the uncoordinated carboxylate oxygen atoms (O2 and O4) in **3** lie to the same side of the central square plane.

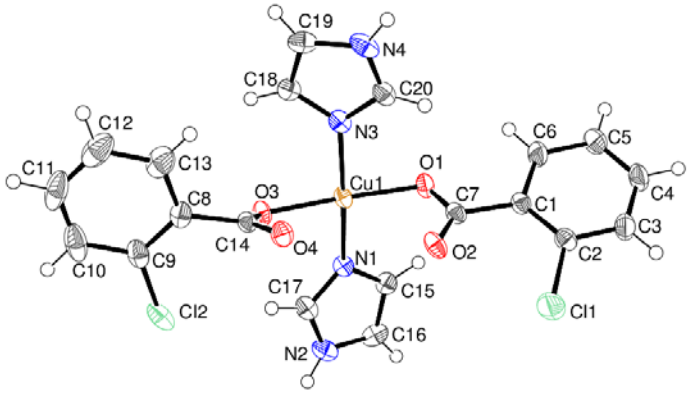

Figure 5: The molecular structure of **3** showing 50% displacement ellipsoids.

Table 6. Selected bond lengths (A˚) and angles (˚) for complex **3**

Bond Lengths			
Cu1–O3	1.951 (2)	Cu1–O1	1.958 (2)
Cu1–N1	1.976 (3)	Cu1–N3	1.979 (3)
C7–O2	1.235 (4)	C7–O1	1.278 (4)
C14–O4	1.233 (4)	C14–O3	1.278 (4)
Bond Angles			
O3–Cu1–O1	174.85(10)	O3–Cu1–N3	89.99(11)

O3–Cu1–N1	89.64(10)	O1–Cu1–N3	89.93(11)
O1–Cu1–N1	90.95(11)	N1–Cu1–N3	174.23(12)

The packing in **3** features N–HΛO hydrogen bonds, which generate [101] chains (Fig. 6): each pair of adjacent molecules, *A* and *B*, in the chain are linked by two hydrogen bonds (one *A*→*B* and one *B*→*A*) with the uncoordinated carboxylate O2 and O4 atoms acting as acceptors. Within these chains the imidazole rings appear to interact by π–π stacking [centroid–centroid separations = 3.649 (2) Å for inversion-related N1 molecules and 3.789 (2) Å for inversion related N2 molecules]. The chains are cross-linked by weak C–HΛO interactions, which results in a three-dimensional network (Table 7). Unlike **1**, the benzene rings in **3** are not involved in π–π stacking interactions.

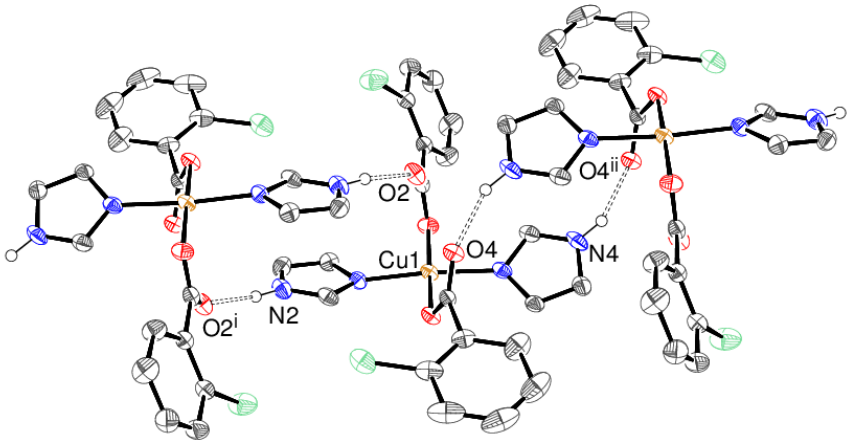

Figure 6: Fragment of the extended structure of **3** showing the formation of [101] chains linked by N–HΛO hydrogen bonds. Symmetry codes as in Table 7.

Table 7: Bond separations (Å) and bond angles (˚) in the complex (**3**)

Donor–H ….. Acceptor	D–H (Å)	H…A (Å)	D–H…A (Å)	D–H…A (º)
N2–H2ΛO2^{i}	0.88	1.96	2.826 (4)	167
N4–H4aΛO4^{ii}	0.88	1.95	2.772 (4)	156
C16–H16ΛO4^{i}	0.95	2.55	3.235 (4)	129
C17–H17ΛCl2	0.95	2.84	3.786 (4)	176
C18–H18ΛO3^{iii}	0.95	2.48	3.337 (4)	150

5. Supplementary material

Crystallographic data for the structures in this paper have been deposited with the Cambridge Crystallographic Data Centre, CCDC, 12 Union Road, Cambridge CB2 1EZ, UK. Copies of the data can be obtained free of charge on quoting the depository numbers CCDC-1543434 (**1**), CCDC-1543435 (**2**) and CCDC-1543436 (**3**) (Fax: +44-1223-336-033; E-Mail: deposit@ccdc.cam.ac.uk, http://www.ccdc.cam.ac.uk).

4. Conclusions

In conclusion, three novel mixed-ligand Cu(II) complexes **1**–**3**, have been synthesized by the reactions of $CuCl_2$. $2H_2O$ and imidazole with the appropriate carboxylate in 1:2:2 molar ratios in aqueous solution. The FT-IR and UV-visible spectroscopic data are consistent with the crystal structures and with previous literature. In all the complexes **1-3**, the imidazole moiety coordinates to Cu(II) center with the nitrogen that has no H atom. In terms of the crystal structures, the presence of a coordinated H_2O molecule in **1,** a *p*-substituted NH_2 and *o*-substituted Cl groups in carboxylate moieties in **2** and **3**, respectively, gives rise to different 'weak' interactions in addition to hydrogen bonding (N–HΛO, O–HΛO). These relatively weak interactions (C–HΛO, N–HΛπ, C–HΛπ and π–π) also appear to play an important role in establishing the packing for **1**–**3**.

So far as we are aware, complexes **1** and **3** represent the first ligand combinations of imidazole + the cinnamate and 4-amino benzoate anions, respectively with copper as the metal ion. A search of the Cambridge Database (updated to June 2017) yielded 11 'hits' for complexes of copper with the cinnamate anion and other ligands and 21 hits for copper + *para*-amino benzoate + other ligands. Complex **2** has an interesting analogue in terms of $[Cu(Himz)_3(clba)_2]$ [14], in which three, rather than two imidazole molecules coordinate to the metal ion to result in a near regular trigonal bipyramidal geometry for the copper ion (with both $clba^{1-}$ ligands in equatorial sites). Otherwise, there are no fewer than 59 structures of complexes containing copper, $clba^{1-}$ and other ligands deposited to the Cambridge Database. The thermal characteristics of complexes **1-3** have also been studied. It is observed that the coordinated water (complex **1**) is removed first, and then carboxylate moiety is eliminated. Removal of imidazole groups occurs in the subsequent step.

References

[1] R.N. Patel, N. Singh, K.K. Shukla, U.K. Chauhan, Spectrochimica Acta Part A: Molecular and Biomolecular Spectroscopy 61 (2005) 287-297.

[2] Z. Heren, C. Keser, C.C. Ersanlı, O.Z. Yeşilel, O. Büyükgüngör, Zeitschrift für Naturforschung B (2006) 1072.

[3] W. WoŁodkiewicz, J. Coord. Chem. 55 (2002) 727-734.

[4] T. Otieno, M.J. Hatfield, S.L. Asher, A.I. McMullin, B.O. Patrick, S. Parkin, Synth. React. Inorg. Met.-Org. Chem. 31 (2001) 1587-1598.

[5] D.L. McFadden, A.T. McPhail, C.D. Garner, F.E. Mabbs, J. Chem. Soc., Dalton Trans. (1975) 263-268.

[6] R.-Q. Zhu, W. Zhang, Z. Anorg. Allg. Chem. 639 (2013) 1274-1278.

[7] J. Casanova, G. Alzuet, J. Borras, O. Carugo, J. Chem. Soc. Dalton Trans. (1996) 2239-2244.

[8] C. Benelli, R. Bunting, D. Gatteschi, C. Zanchini, Inorg. Chem. 23 (1984) 3074-3076.

[9] L.D. Luca, Current medicinal chemistry 13 (2006) 1-23.

[10] P. Gupta, S. Hameed, R. Jain, European Journal of Medicinal Chemistry 39 (2004) 805-814.

[11] M. Puchoňová, J. Švorec, Ľ. Švorc, J. Pavlik, M. Mazúr, Ľ. Dlháň, Z. Růžičková, J. Moncoľ, D. Valigura, Inorg. Chim. Acta 455 (2017) 298-306.

[12] A.L. Abuhijleh, C. Woods, Inorg. Chim. Acta 194 (1992) 9-14.

[13] G.Y.S.K. Swamy, P. Sivanarayanan, B. Sridhar, L.R. Joshi, J. Coord. Chem. 69 (2016) 1602-1617.

[14] S.S. Batool, S. Ahmad, I.U. Khan, Ejaz, W.T.A. Harrison, J. Struct. Chem. 56 (2015) 387-391.

[15] S.S. Batool, S.R. Gilani, M.N. Tahir, A. Siddique, W.T.A. Harrison, J. Struct. Chem. 57 (2016) 1176-1181.

[16] S.S. Batool, S.R. Gilani, M.N. Tahir, W.T.A. Harrison, J. Struct. Chem. 57 (2016) 991-996.

[17] G.M. Sheldrick, Acta Crystallographica Section C: Structural Chemistry 71 (2015) 3-8.

[18] K. Nakamoto, Infrared and Raman spectra of inorganic and coordination compounds, 5 ed., John Wiley and Sons, 1997.

[19] S.S. Batool, S.R. Gilani, M.N. Tahir, W.T.A. Harrison, Z. Anorg. Allg. Chem. 642 (2016) 1364-1368.

[20] S.S. Batool, S.R. Gilani, M.N. Tahir, T. Rüffer, J. Mol.Struct. 1148 (2017) 7-14 https://doi.org/10.1016/j.molstruc.2017.07.014.

[21] G. Deacon, R. Phillips, Coord. Chem. Rev. 33 (1980) 227-250.

[22] A. Taha, A. Farag, A. Ammar, H. Ahmed, Spectrochimica Acta Part A: Molecular and Biomolecular Spectroscopy 130 (2014) 494-501.

[23] S.G. Baca, M.T. Reetz, R. Goddard, I.G. Filippova, Y.A. Simonov, M. Gdaniec, N. Gerbeleu, Polyhedron 25 (2006) 1215-1222.

[24] B. Morzyk-Ociepa, E.Różycka-Sokołowska,D. Michalska J. Mol.Struct. 1028 (2012) 49-56.

[25] K. S. Vinod, S. Periandy, M. Govindarajan Spectrochim. Acta Part A: Molecular and Biomolecular Spectroscopy 136 (2015) 808-817.

[26] R. Świsłocka, M. Kalinowska, W. Ferenc, J. Sarzyński, W. Lewandowski, Cent. Eur. J. Chem. 10. 4 (2012) 1095-1105.

[27] R. Świsłocka, M. Samsonowicz, E. Regulska, W. Lewandowski, J. Mol.Struct. 792 (2006) 227-238.

[28] N.B. Sundaraganesan, J. Dominic, T. Radjakoumar. (2009). http://nopr.niscair.res.in/handle/123456789/4075.

[29] S.S. Massoud, F.R. Louka, R.N. David, M.J. Dartez, Q.L. Nguyn, N.J. Labry, R.C. Fischer, F. A. Mautner, Polyhedron 90 (2015) 258-265.

[30] F.A. Mautner, M. Koikawa, M. Mikuriya, E.H. Harrelson, S.S. Massoud, Polyhedron 59 (2013) 17-23.

[31] F.A. Mautner, J.H. Albering, E.V. Harrelson, A.A. Gallo, S.S. Massoud, J. Mol. Struct. 1006 (2011) 570-575.

[32] L.M. Araya, J.A. Vargas, J.A. Costamagna, Transition Met. Chem. 11 (1986) 312-316.